Interactions between Individual Carbon Nanotubes Studied by Rayleigh Scattering Spectroscopy

Feng Wang,[1] Matthew Y. Sfeir,[2] Limin Huang,[3] X. M. Henry Huang,[4] Yang Wu,[1] Jaehee Kim,[1] James Hone,[4]
Stephen O'Brien,[3] Louis E. Brus,[2] and Tony F. Heinz[1]

[1]*Departments of Physics and Electrical Engineering, Columbia University, New York, New York 10027, USA*
[2]*Department of Chemistry, Columbia University, New York, New York 10027, USA*
[3]*Department of Applied Physics and Applied Mathematics, Columbia University, New York, New York 10027, USA*
[4]*Department of Mechanical Engineering, Columbia University, New York, New York 10027, USA*

The electronic properties of single-walled carbon nanotubes (SWNTs) are altered by intertube coupling whenever bundles are formed. These effects are examined experimentally by applying Rayleigh scattering spectroscopy to probe the optical transitions of given individual SWNTs in their isolated and bundled forms. The transition energies of SWNTs are observed to undergo redshifts of tens of meVs upon bundling with other SWNTs. These intertube coupling effects can be understood as arising from the mutual dielectric screening of SWNTs in a bundle.

Single-walled carbon nanotubes (SWNTs), with diameters of nanometers and lengths up to millimeters, are prototypical one-dimensional (1D) systems [1–3]. This 1D character leads to many unique physical phenomena in SWNTs [4,5], including greatly enhanced Coulomb interactions [6–10]. Because all the carbon atoms of a SWNT lie on its surface, the physical properties of SWNTs exhibit a strong dependence on the local environment [11]. In particular, the interactions between SWNTs in close proximity with one another, and the corresponding changes in their electronic structure, have received much attention [12–19]. In addition to the inherent interest in understanding interacting 1D systems, intertube interactions are of substantial technological importance because SWNTs naturally form bundles in typical syntheses [20,21]. In this Letter, we investigate the role of intertube interactions on the excited-state properties of individual SWNTs. Using Rayleigh scattering spectroscopy, we compare optical transitions of individual SWNTs in both isolated and bundled form. We find that the optical response of a small nanotube bundle is, to a good approximation, just the sum of the contributions from each of the constituents. The optical transition energies are, however, redshifted by several tens of meV. In contrast to previous studies of bundling effects in ensemble samples [17,18,22], we observe no broadening of the spectral features in our single-tube measurements. The experimental results can be understood as the consequence of the dielectric screening provided by an adjacent nanotube. The dielectric screening acts to reduce the many-body interactions of charges in each SWNT, leading to a redshift in the optical transition energies without line broadening. The present investigations complement recent studies on spectral shifts in nanotubes associated with changes in their local physical and chemical environment [18,19,23,24].

The experimental apparatus of Rayleigh scattering spectroscopy has been described previously [25]. In brief, we generate supercontinuum radiation, a source of high-brightness white light, by passing femtosecond pulses from a mode-locked Ti:sapphire laser through a micro-structured optical fiber. This radiation is focused on the nanotube with a spot size of $\sim 2 \ \mu m^2$. The elastically scattered light from the nanotube is collected in a dark-field configuration and analyzed with a spectrometer equipped with a 2D array detector.

The Rayleigh scattering intensity depends on the dielectric function and geometric size of the scattering object. Approximating a SWNT as an infinite cylinder, we obtain a scattering cross section per unit length of $\sigma(\omega) \propto r^4(\omega/c)^3|\varepsilon(\omega) - 1|^2$, where ω is the frequency of the light, r the nanotube radius, and $\varepsilon(\omega)$ the frequency-dependent dielectric function. The Rayleigh scattering spectra reflect a nanotube's dielectric response and, hence, probe the electronic transitions. Below we present Rayleigh spectra corrected for the $(\omega/c)^3$ factor to reflect directly the dielectric function of the structure. The simplicity of the Rayleigh response is in contrast with that of Raman excitation spectroscopy in which the observation of electronic transitions can be complicated by the influence of electron-phonon interactions [26]. In our measurements, suspended SWNTs are grown across slit structures by chemical vapor deposition (CVD). The slit structures (100 $\mu m \times 1$ mm) are prepared by standard photolithography and wet etching techniques [27]. For the CVD growth of SWNTs, we use a 1-nm-thick Co film as the catalyst and ethanol as the feedstock gas. This procedure yields aligned SWNTs of lengths extending into the mm range [2]. Most of the SWNTs that cross the slit, whether as individual nanotubes or as bundles, maintain the same composition throughout. Sometimes, however, two nanotubes merge into one structure midway across the slit to form a Y-junction structure [Figs. 1(a) and 1(b)]. Alternatively, the growth of part of a nanotube bundle may stop part way across the slit, with only one of the individual constituent nanotubes reaching across the entire gap [Fig. 2(a)]. Because the light source in our Rayleigh mea-
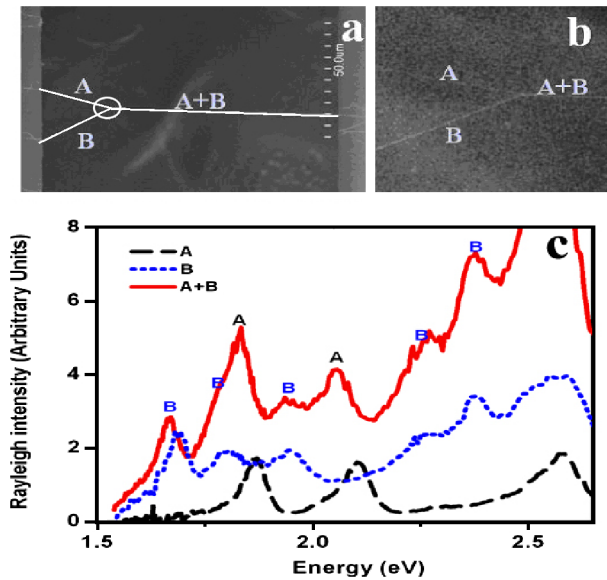
FIG. 1 (color online).   Rayleigh spectra at different positions in a nanotube Y junction. (a) Scanning electron micrograph (SEM) image of the Y junction where two nanotube structures (A and B) merge together ($A + B$). The positions of the nanotubes have been highlighted with white lines. (b) High-resolution SEM image of the junction area indicated by the circle in (a). (c) Rayleigh spectra of structure A (black dashed curve), structure B (blue dotted curve), and the combination $A + B$ (red solid curve). Structure A is an isolated semiconducting nanotube with diameter of $\sim$1.9 nm; B is a small bundle of nanotubes. The composite $A + B$ structure exhibits features of both constituents, with peaks arising from structures A and B marked correspondingly. The resonances in SWNT A are redshifted by 35 and 47 meV in the $A + B$ structure. The redshifts for transitions in structure B are smaller.

surements is tightly focused, we are able to examine the electronic transitions at different spatial locations by adjusting the position of the optical probe beam along the 100 μm width of the slit. This capability permits us to study an individual SWNT in both its isolated and bundled form.

Shown in Fig. 1(c) are the Rayleigh scattering spectra for the nanotube Y junction of Figs. 1(a) and 1(b). In this structure, two nanotubes grow from the left edge, meet in the middle of the slit, and merge into a bundle that extends to the right edge of the slit. By recording Rayleigh spectra at different spatial locations, we are able to probe the response of the two nanotube structures (A and B) separately, as well as of the composite structure ($A + B$). The Rayleigh spectrum of A [black curve in Fig. 1(c)] shows two sharp well-separated resonances in the visible spectral range. From these features, we deduce that we are probing an individual semiconducting SWNT with diameter $\sim$1.9 nm [25]. Structure B, on the other hand, displays higher scattering intensity, more peaks in the spectrum, and a larger background in its Rayleigh spectrum [blue curve in Fig. 1(c)]. These characteristics indicate that structure B is a nanotube bundle, rather than an individual SWNT. The
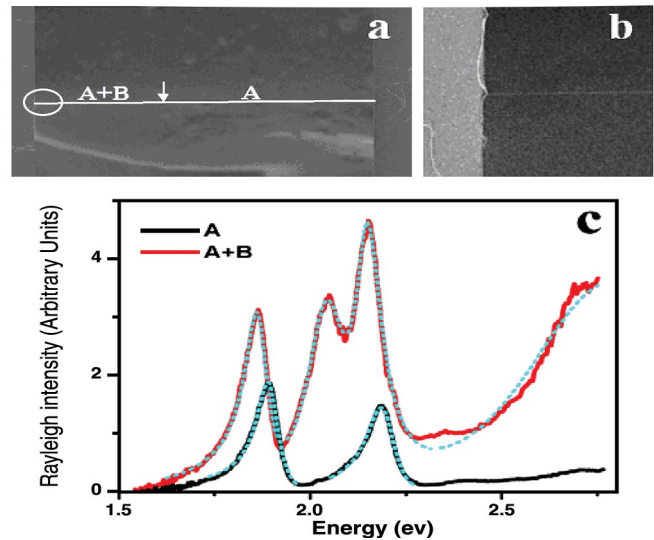
FIG. 2 (color).   Rayleigh spectra of a SWNT and a two-tube bundle containing this SWNT. (a) SEM image of the nanotube structure, with nanotubes highlighted by white lines. The arrow indicates the position of the transition between the two-tube bundle $A + B$ and the individual tube A. (b) Detailed SEM image of the circled area showing the formation of the two-tube bundle at the edge of the slit. (c) Rayleigh spectra of the individual semiconducting SWNT A of 1.8-nm diameter (black curve) and the two-tube bundle $A + B$ (red curve). The dotted lines are generated using the model for the Rayleigh spectra discussed in the text. Redshifts of 29 and 48 meV for the SWNT transitions at 1.897 and 2.196 eV, respectively, arise from the SWNT's interaction with the adjacent SWNT. No changes in the optical transition linewidths are observed.

Rayleigh spectrum of the merged structure ($A + B$) clearly arises from the sum of the separate responses of A and B, as we can attribute all of the resonances of $A + B$ to features in the individual A and B tubes [Fig. 1(c)]. The energies of the electronic resonances in the $A + B$ bundle are, however, redshifted compared with those in the separated structures. For individual SWNT A, the two Rayleigh resonances at 1.870 and 2.108 eV are redshifted by 35 and 47 meV, respectively. The redshifts of the resonances present in bundle structure B are considerably smaller, with an average shift of just $\sim$8 meV. The weaker effect of an individual nanotube on a bundle compared to the reverse case is consistent with the fact that there is a lesser change in the local environment for the bundle.

Another type of nanotube structure allowing for controlled examination of intertube coupling effects is shown in Figs. 2(a) and 2(b). Here only one component of a two-tube bundle extends across the entire slit. The other nanotube, which grows from the left edge [Fig. 2(b)], ends abruptly in the gap [arrow in Fig. 2(a)]. Depicted in Fig. 2(c) are Rayleigh spectra obtained in the two regions of the sample [Fig. 2(a)]. Spectrum A corresponds to an individual semiconducting SWNT of 1.8-nm diameter, while spectrum ($A + B$) reflects a two-tube bundle of SWNTs. From a comparison of the two spectra, we find

that the energies of the Rayleigh peaks of individual SWNT *A* are redshifted by 27 and 37 meV in forming bundle (*A* + *B*).

Further results for nanotube structures similar to that in Fig. 2(a) are shown in Fig. 3. The black traces are Rayleigh spectra of individual SWNTs; the red curves are obtained from the small bundles containing the same SWNTs. In all of the spectra, we can identify the features of the isolated SWNTs in the bundles, but with redshifts in the Rayleigh peak positions ranging from 20 to 56 meV. The induced redshifts are present for both semiconducting and metallic SWNTs: the individual nanotubes of Figs. 3(a) and 3(c) are representative of metallic SWNTs, while the Rayleigh scattering features in Figs. 3(b) and 3(d) are consistent with semiconducting SWNTs.

In order to relate the observed intertube effects to the optical transitions, we consider the Rayleigh spectra of the SWNT structures in greater detail. The electronic bands in SWNTs can be understood using zone folding of the graphene electronic structure as a starting point [4]. Associated with each quantized angular momentum in the SWNT there is an electronic band. This band picture is modified when the strong Coulomb interactions in the 1D SWNTs are taken into account [6–8,28–31]. The electron-electron interactions in a carbon nanotube have two important consequences for the optical properties: they enlarge the band gaps and they lead to the formation of exciton states associated with each band. It has been shown that the exciton states dominate the linear optical transitions in semiconducting SWNTs [6–9], although the case for metallic nanotubes is presently less clear.

Since each exciton state has a discrete energy level, the dielectric function of the nanotube $\varepsilon(\omega)$ can be described as the sum of Lorentzian line shapes with a constant nonresonant (NR) background contribution ε_{NR}: $\varepsilon = \varepsilon_{NR} + \sum_i A_i/(\omega_i^2 - \omega^2 - i\omega\gamma_i)$. Here A_i, ω_i and γ_i are, respec-

tively, the strength, transition frequency, and dephasing rate of the *i*th exciton transition.

Figure 2(c) shows fits to the experimental Rayleigh scattering data. We obtain exciton transition energies of 1.897 and 2.196 eV with respective linewidths of 71 and 87 meV for single-tube *A*. For the two-tube bundle (*A* + *B*), we obtain a good fit of the Rayleigh spectrum by including four distinct exciton transitions. The two exciton transitions present in the isolated SWNT (*A*) now have transition energies of 1.868 and 2.148 eV, with linewidths of 71 and 85 meV. The transition energies are seen to be redshifted by 29 and 48 meV, respectively, but the linewidths remain essentially unchanged upon bundling. While redshifts of comparable magnitude have been previously reported in ensemble studies of bundling, the behavior of the linewidth is quite different. In the ensemble measurements, broadening of the spectral features by a factor of 2–3 upon bundling is observed [17]. This comparison underscores the utility of probing carbon nanotubes at the single-tube level.

To understand the physical origin of the redshifts of transition energies observed for the nanotube bundles, we compare two types of intertube interactions that have been previously discussed in the literature. One arises from the direct coupling of the electronic states in adjacent nanotubes from overlap of their electron wave functions [12,14,15]. The second type of interaction is an electrodynamical coupling in which Coulomb interactions in a SWNT are modified by the dielectric screening induced by other adjacent nanotubes [18].

To analyze the first type of interaction, we follow the treatment of Maarouf *et al.* [14] for the quantum coupling between adjacent nanotubes. For a single-particle band state, only states with the same wave vectors along the nanotube have nonzero coupling. The tunneling between these states is characterized by a matrix element *t*, estimated to be ∼7 meV in nanotubes of diameters around 2 nm [14]. For coupled electronic states with an energy difference of ΔE, typically hundreds of meV for SWNTs of different chirality, perturbation theory yields tunneling-induced energy shifts of $\sim t^2/\Delta E < 1$ meV. In our measurements, we record energies of exciton states, but these should track the corresponding single-particle states and exhibit similar shifts. Therefore quantum tunneling between adjacent SWNTs cannot account for the observed shifts of tens of meVs. The direct coupling mechanism also cannot explain the consistent redshift seen experimentally; direct coupling produces energy shifts of either sign, depending on the relative position of transition energies in the adjacent SWNTs. A model based on such direct coupling [15] has previously been invoked to explain the broadening of optical transitions measured in ensemble samples upon bundling [17]. The lack of analogous broadening in our studies of individual nanotubes, as discussed above, suggests that the broadening may be due to the inhomogeneity in the ensemble samples.

FIG. 3 (color online).   Rayleigh spectra of four separate nanotube structures similar to that of Fig. 2(a). Both Rayleigh scattering of individual SWNTs (black solid curves) and bundles containing these tubes (red dashed curves) are displayed. The resonances of the SWNTs are present in the bundled structures (vertical lines), but at redshifted energies.

Let us now consider the electrodynamical coupling between nanotubes in a bundle. The electron-electron interaction in a SWNT can be partially screened by an adjacent nanotube. Such dielectric screening can have significant effects in 1D structures like SWNTs since many-body interactions are inherently strong in 1D and much of the electric field of a charge extends outside of a nanotube. As mentioned above, the Coulomb interaction increases all the interband energy separations in SWNTs and also leads to the formation of excitons. Theoretical studies predict that the gap-opening effect dominates over the excitonic effect, so that the net effect of Coulomb interactions is an increase in the transition energies [6,8]. Thus, when the effective strength of Coulomb interaction is reduced by intertube screening, a redshift in the transition energies will result. This behavior is analogous to solvatochromic effects in molecules in solution, which have been extensively studied for π-conjugated systems [32]. A similar dielectric screening has also been observed for optical transitions in molecular crystals [33]. To estimate the effect of dielectric screening, we consider the SWNTs as 2-nm dielectric cylinders with a dielectric function of $\varepsilon = 10$ [34], a value typical of bulk semiconductors. We solve numerically the Coulomb potential produced by a thin disk of charge in an isolated nanotube and in one with an adjacent nanotube. We find that the Coulomb potential is reduced by approximately 20% due to the dielectric screening induced by a single adjacent nanotube [35]. Because the many-body effects lead to changes in the excited-state energies of SWNTs of several hundred meV [6–9], such a reduction in the effective Coulomb interaction should induce redshifts of tens of meV, in agreement with our experimental observations. Of course, the numerical value of redshift of a given transition will depend on the precise nature of the many-body interactions within the specific SWNT, as well as on the effectiveness of the dielectric screening induced by adjacent tubes.

In conclusion, we have shown that Rayleigh scattering spectroscopy of suspended nanotube structures provides a means of directly probing intertube interactions in SWNTs. Such intertube coupling leads to redshifts of tens of meV in the energies of optical transitions. Because the energy shifts are comparable to or larger than thermal energies at room temperature, tube-tube interactions are expected to induce appreciable changes in other SWNT properties when they form bundles. The study of tube-tube interactions also addresses the broader questions of the effect of the environment on the behavior of SWNTs. In particular, our proposed mechanism for the intertube interactions—one based on dielectric screening—is quite general and suggests a convenient approach to tune the electronic properties of a specified nanotube.

[1] K. Hata *et al.*, Science **306**, 1362 (2004).
[2] L. M. Huang *et al.*, J. Phys. Chem. B **108**, 16 451 (2004).
[3] S. M. Huang *et al.*, Nano Lett. **4**, 1025 (2004).
[4] R. Saito, G. Dresselhaus, and M. S. Dresselhaus, *Physical Properties of Carbon Nanotubes* (Imperial College Press, London, 1998).
[5] Z. Yao, C. Dekker, and P. Avouris, Top. Appl. Phys. **80**, 147 (2001).
[6] T. Ando, J. Phys. Soc. Jpn. **66**, 1066 (1997).
[7] V. Perebeinos, J. Tersoff, and P. Avouris, Phys. Rev. Lett. **92**, 257402 (2004).
[8] C. D. Spataru *et al.*, Phys. Rev. Lett. **92**, 077402 (2004).
[9] F. Wang *et al.*, Science **308**, 838 (2005).
[10] J. Maultzsch *et al.*, Phys. Rev. B **72**, 241402 (2005).
[11] J. Kong *et al.*, Science **287**, 622 (2000).
[12] P. Delaney *et al.*, Nature (London) **391**, 466 (1998).
[13] Y. K. Kwon, S. Saito, and D. Tomanek, Phys. Rev. B **58**, R13314 (1998).
[14] A. A. Maarouf, C. L. Kane, and E. J. Mele, Phys. Rev. B **61**, 11 156 (2000).
[15] S. Reich, C. Thomsen, and P. Ordejon, Phys. Rev. B **65**, 155411 (2002).
[16] M. Ouyang *et al.*, Science **292**, 702 (2001).
[17] M. J. O'Connell, S. Sivaram, and S. K. Doorn, Phys. Rev. B **69**, 235415 (2004).
[18] C. Fantini *et al.*, Phys. Rev. Lett. **93**, 147406 (2004).
[19] D. A. Heller *et al.*, J. Phys. Chem. B **108**, 6905 (2004).
[20] A. Kis *et al.*, Nat. Mater. **3**, 153 (2004).
[21] R. H. Baughman, A. A. Zakhidov, and W. A. de Heer, Science **297**, 787 (2002).
[22] M. J. O'Connell *et al.*, Science **297**, 593 (2002).
[23] T. Hertel *et al.*, Nano Lett. **5**, 511 (2005).
[24] P. Finnie, Y. Homma, and J. Lefebvre, Phys. Rev. Lett. **94**, 247401 (2005).
[25] M. Y. Sfeir *et al.*, Science **306**, 1540 (2004).
[26] M. Machon *et al.*, Phys. Rev. B **71**, 035416 (2005).
[27] M. J. Madou, *Fundamentals of Microfabrication: The Science of Miniaturization* (CRC Press, Boca Raton, Fla., 2002).
[28] H. B. Zhao and S. Mazumdar, Phys. Rev. Lett. **93**, 157402 (2004).
[29] C. L. Kane and E. J. Mele, Phys. Rev. Lett. **93**, 197402 (2004).
[30] E. Chang *et al.*, Phys. Rev. Lett. **92**, 196401 (2004).
[31] T. G. Pedersen, Phys. Rev. B **67**, 073401 (2003).
[32] P. Suppan, J. Photochem. Photobiol., A **50**, 293 (1990).
[33] E. V. Tsiper and Z. G. Soos, Phys. Rev. B **68**, 085301 (2003).
[34] M. F. Lin, Phys. Rev. B **62**, 13 153 (2000).
[35] See EPAPS Document No. E-PRLTAO-96-059617 for supplementary information for the Letter. For more information on EPAPS, see http://www.aip.org/pubservs/epaps.html.